Implementation and Initial Operation of an Adaptive Plasma Density Controller at JET.

H. E. O. Brelén, T. Budd, J. Ehrenberg, M. Gadeberg, C. Ryle

JET Joint Undertaking
Abingdon, Oxfordshire OX14 3EA, England

An adaptive controller has been tried in the plasma density feedback system at JET in an effort to improve the control performance as produced by the present conventional controller. Changing plant dynamics calls for retuning of the controller to retain the required performance of the control system. This controller tuning must in the conventional case be done manually. In the adaptive controller, the retuning process is automated and runs in parallel with the control function. The adaptive controller was implemented and commissioned for on-line operation. Experience from the use of the controller and its performance is presented and analysed. It is the first time this controller technology has been applied at JET

1. REQUIREMENTS

The new plasma density controller was designed under the following performance requirements:

- 1.5 - 2 seconds settling time to within 1% control accuracy following a stepwise change in the reference signal.
- maintained stability and recovery within 20 s to above performance figures due to sudden changes over the whole expected plant parameter range.
- maximum 5% overshoot following a stepwise change in the reference signal.
- disturbance rejection factor of at least 20.
- no steady state control deviation.

2. CONTROLLER

A controller with the following control law was introduced:

$$R \cdot u = T \cdot x - S \cdot y \qquad (1)$$

where R, T and S are polynomials of the discrete time shift operator z. x represents the requested plasma density, y the real plasma density and u the actuation signal to the gas introduction. With the plant transfer function B/A, the closed loop transfer function for the control loop is:

$$\frac{y}{x} = \frac{T \cdot B}{A \cdot R + S \cdot B} \qquad (2)$$

3. DESIGNER

Required control performance is translated to required pole locations for the closed loop transfer function, equation 2. The coefficients in the controller polynomials, R and S, are calculated in the designer routine so that for any plant polynomials, B and A, the required pole locations are obtained.

The controlled system has zeros in common with the plant one of which can approach z=1. Its effect is made worse by the fact that, unlike the open loop transfer function, the controlled system does not have an integrator pole to reduce it. Overshoots caused by this zero can be several times larger than the steady state level. By making one of the poles of the controlled system coincide with this zero, that is the zero in B should also be a zero in AR+BS, its effect is cancelled and the intended system performance should be seen.

The situation is complicated by the fact that the plant zero and poles move due to changing plant parameters. In order to maintain the performance of the system, keeping its poles in the required positions including the one cancelling the zero, the calculation of the coefficients of the controller polynomials R and S have to be repeated at each sampling occasion, with the latest estimate of the A and B polynomials.

Finally the polynomial T is used to produce zeros for avoiding unnecessary delays in the controlled system.

4. IDENTIFIER

The identifier produces estimates of the coefficients in the plant polynomials A and B that are necessary for the above controller design. The recursive least square identifier is chosen for this purpose, and the algorithm for this is:

$$\theta_{n+1} = \theta_n + K_{n+1}(y_{n+1} - \varphi_{n+1}^T\theta_n) \qquad (3)$$

where

$$K_{n+1} = \frac{P_n}{\beta}\varphi_{n+1}\left(\frac{1}{1-\beta} + \varphi_{n+1}^T\frac{P_n}{\beta}\varphi_{n+1}\right)^{-1} \qquad (4)$$

$$P_{n+1} = \frac{1}{\beta}(I - K_{n+1}\varphi_{n+1}^T)P_n \qquad (5)$$

where y is the plant output, φ contains recent and historic values of the y and u variables from the plant and θ is the identified parameter vector. $\varphi^T\theta$ is thus the identifier's estimate of the plant output. β determines the length of the identifier's 'forget function'. Figure 1 shows the structure of the adaptive controller. A more detailed description of the controller can be found in [1].

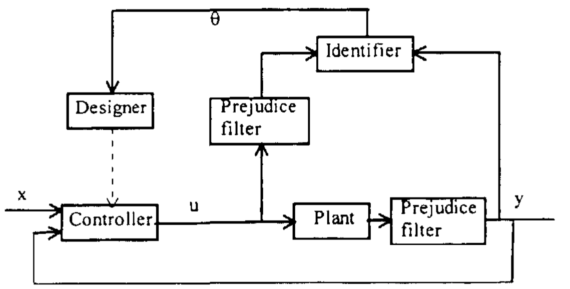

Figure 1: Flow chart of adaptive controller with prejudice filters.

5. ROBUSTNESS

A crucial point in the implementation of the adaptive controller is the robustness of its identifier. To avoid distracting the identifier with uncorrelated data it is only made to operate as long as plasma is being formed with confidence. The controller action is however executed at all times, be it with fixed parameters when the identifier is not running. In order to protect the identifier from the strong uncorrelated influence on the density from neutral beams, radiofrequent heating, X-point formation and plasma touching the limiters, the following modification was made to equation (3).

$$\theta_{n+1} = \theta_n + K_{n+1}\frac{e}{1+\alpha|e|} \qquad (6)$$

where e stands for the identification error $y_{n+1}-\varphi^T_{n+1}\theta_n$ and α is a tuning parameter.

In order to safeguard the identifier from being distracted by high frequency poles and zeros, also so called prejudice filters were introduced as indicated in Figure 1.

6. RESULTS FROM FIRST ON-LINE TESTS.

The adaptive controller was brought on-line in May 1995 and was operational during 30 successive pulses leading up to the 1995 shutdown. The experience from its operation was very positive.

Results from pulse 35253 during which the adaptive controller was in control of the plant is here used to show the performance of the controller. At about 8 s into the pulse the X-point was formed, see Figure 2, which drains the plasma of particles. In order to avoid an excessive inflow of gas as a result of the anticipated controller reaction to this loss of density, a certain allowance was edited in the reference waveform. The large density peak following at 12 s is due to a short pulse of RF power, altogether a good test of the adaptive controller.

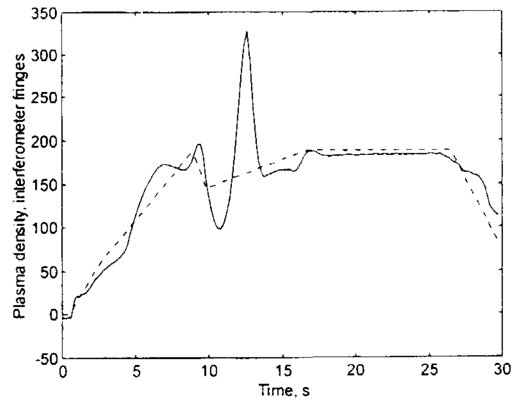

Figure 2: Reference signal, dashed line, and controlled plasma density signal, continuous line..

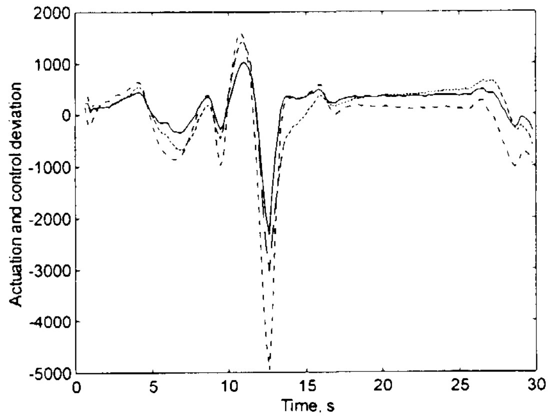

Figure 3: Plant actuation signal, dashed line. Plant actuation with new weighting function, dotted line. Control deviation magnified with a factor 30, continuous line.

Figure 3 shows the actuation in comparison to the plasma density deviation (scaled up a factor of 30 to show on the same plot). It is apparent how the simultaneous redesign of the controller has changed the "proportionality" to the deviation signal. The controller response to the X-point formation was, despite the allowance in reference waveform, a prompt and nearly full opening of the valve. The RF pulse caused an actuation 2.5 times the full range. (Negative actuations are limited to zero before being sent to the plant.)

Figure 4 shows the identification error relative to the real density signal. The large excursions in the beginning of the pulse when the identifier was engaged is partly due to the initial parameter values not being accurate and partly due to the real density signal being quite low. The relative identification error stays mostly within 5 percent, but increases of course during disturbances like the RF pulse. The identification accuracy seems to be sufficient as far as the pole placement is concerned. The estimated gain would if it were obtained more accurately and faster, possibly have led to a more accurate control in the stationary part, between 18 and 26 s, of the pulse.

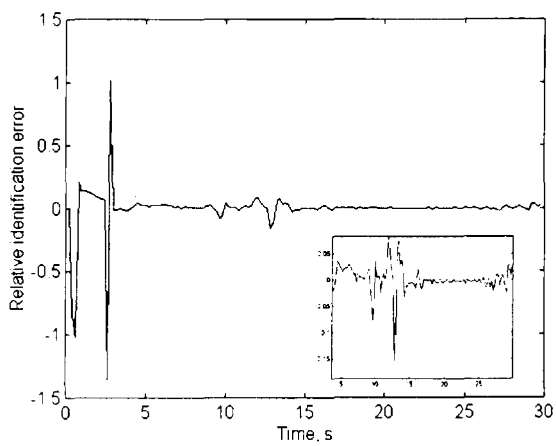

Figure 4: Relative identification error

Time graphs showing how the identified parameters associated with the numerator and the denominator of the transfer function developed during the pulse are given in Figure 5 and Figure 6 respectively. All parameters are of course affected by the X-point and the RF pulse but no worse than what is tolerable for the controller as a whole. It is also conceivable that the X-point formation and the RF pulse caused some change in the plant giving rise to some true change in the identified transfer function.

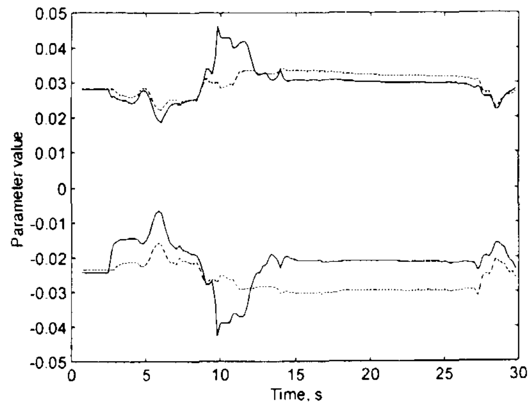

Figure 5: Numerator parameters as identified during the pulse continuous line and simulated with suggested identification error weighting function for the same pulse dashed line.

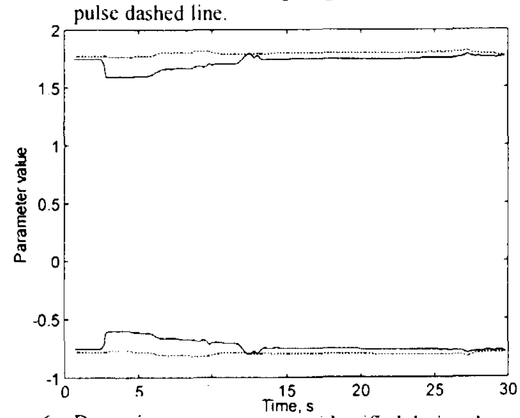

Figure 6: Denominator parameters as identified during the pulse continuous line and simulated with suggested identification error weighting function for the same pulse dashed line.

The movements of the identified transfer function's zero and poles during the pulse are shown in Figure 7 and Figure 8 respectively. The pattern of the these zero and pole locations are as expected and are also comparable to what is experienced from all other pulses on which the identifier has been operated.

Finally, step responses from every fifth identified transfer function are presented in Figure 9. A fairly wide range of dominating time constants and gains is displayed. A few very long time constant responses are just distinguishable among the majority of responses which tend to show time constants around 4 s. It is also remarkable to see how the gain of the identified transfer functions varied by a factor two.

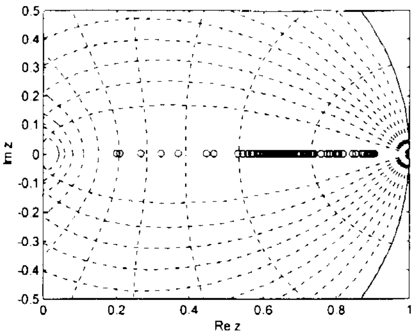

Figure 7: Locations of identified zeros during the pulse.

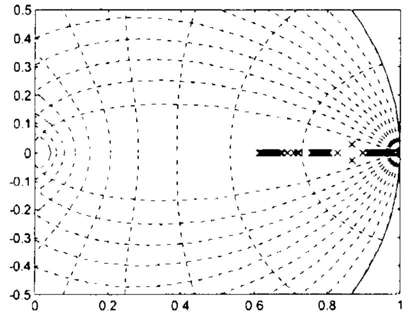

Figure 8: Identified pole locations during the pulse

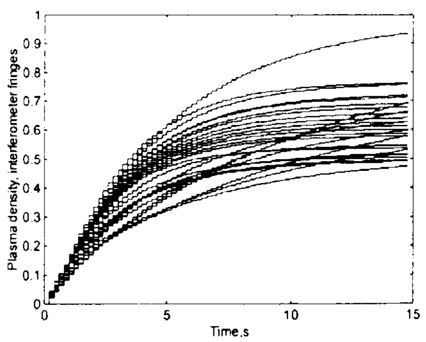

Figure 9: Unit stepresponses from every fifth identified model

7. IMPROVING THE CONTROL ACCURACY.

Even though the plasma density is nearly stationary at times, as between 18 and 26 s in the pulse above see Figure 2, parametric changes are most likely taking place throughout the pulse. Decreasing gas pressures in the reservoirs is experienced as loss of gain in the valves and also the condition of the vessel wall keeps changing. This ongoing drift of the parameters causes the identifier to lag behind the true parameter values. An average identification error of less than half a percent is just visible in Figure 4. Some drift in the identified parameters during stationary plasma density can be distinguished in Figure 5.

All identification errors greater than zero are weighted down in its present implementation, Equation 6, reducing the rate of the identification. It would be useful if this weighting function were lifted up to one for small errors, say a few fringes which seems to be adequate in this context, but still have a strong discrimination of large errors. For this purpose the so far used weighting function is replaced with the following:

$$\frac{1}{1+\delta\cdot e^{4}} \qquad (7)$$

where δ is a tuning parameter nominally set to 0.01.

The identifier run off-line on the plant signals from the same pulse with the new weighting function makes a significant difference to the identified parameter values as indicated in Figure 5 and in Figure 6. Consequently the controller design was influenced so that its plant actuation signal changed to what is shown as the dotted line in Figure 3. The new actuation suggests that the control deviation would have been reduced. It should be remembered though that this is the result from an off line open loop simulation and that all signals would have been different in a real closed loop case.

8. CONCLUSION

The adaptive controller appears to perform as specified in almost all aspects. It is stable, it does not show any oscillations or excessive overshoots and it settles within the prescribed time. The adaptive process shows robustness to disturbances and speedy recovery. However, the plasma density deviation to a constant reference is not completely eliminated, as can be seen between 18 s and 25 s in Figure 2. The remaining deviation is negligible from a practical operations point of view but is nevertheless of some interest and will be attended to further.

9. REFERENCE

1. H.E.O. BRELÉN, "An Adaptive Plasma Density Controller at Joint European Torus", Fusion Technology, Vol 27, March 1995.